

Instantaneous frequency extraction in time-varying structures using a maximum gradient method

Jing-liang Liu^{1a}, Xiaojun Wei^{*2}, Ren-Hui Qiu^{1b}, Jin-Yang Zheng^{1c}, Yan-Jie Zhu^{2d} and Irwanda Laory^{2e}

¹College of Transportation and Civil Engineering, Fujian Agriculture and Forestry University, Fuzhou, China

²School of Engineering, University of Warwick, Coventry, United Kingdom

(Received April 11, 2018, Revised June 17, 2018, Accepted June 20, 2018)

Abstract. A method is proposed for the identification of instantaneous frequencies (IFs) in time-varying structures. The proposed method combines a maximum gradient algorithm and a smoothing operation. The maximum gradient algorithm is designed to extract the wavelet ridges of response signals. The smoothing operation, based on a polynomial curve fitting algorithm and a threshold method, is employed to reduce the effects of random noises. To verify the effectiveness and accuracy of the proposed method, a numerical example of a signal with two frequency modulated components is investigated and an experimental test on a steel cable with time-varying tensions is also conducted. The results demonstrate that the proposed method can extract IFs from the noisy multi-component signals and practical response signals successfully. In addition, the proposed method can provide a better IF identification results than the standard synchrosqueezing wavelet transform.

Keywords: instantaneous frequency; time-varying structures; maximum gradient; wavelet transform; wavelet ridge

1. Introduction

Civil engineering structures in operation essentially belong to time-varying or nonlinear structures when exposed to service loads or extreme loads (Liu *et al.* 2015). For example, the mass distribution and stiffness of a vehicle-bridge system would constantly change with time when the vehicle passes the bridge. The cable stiffness would also decrease over time due to accumulated damages of a cable-stayed bridge during its service life. For such time-varying structures, it is of great significance to extract time-dependent dynamic parameters, which will benefit engineers for monitoring structural health condition. However, traditional signal processing techniques, including time domain and frequency domain analysis, are based on the assumption that response signals are stationary and linear. Such methods can only capture features in time or frequency domain, without revealing local characters in both time and frequency domains simultaneously (Feng *et al.* 2013). On the other hand, the response signals of time-

varying structures are often nonstationary, which creates challenge to traditional methods. Time-frequency analysis (TFA) is potential to deal with non-stationary signals and has been widely accepted in recent years. The Hilbert transform (HT) is a common approach to study the time-varying dynamic properties (Feldman 1994a, b, Feldman *et al.* 2017). However, to ensure instantaneous frequency (IF) extracted by the HT being meaningful, some restrictive requirements have to be emphasized, i.e., the target signal should be an intrinsic mode function (IMF). Unfortunately, most response signals are not exact IMFs, and that is why HT cannot provide powerful description for time-varying features (Shi *et al.* 2009). In addition, HT is quite sensitive to random noises, thus often leading to an IF curve with blurred and distorted lines. Therefore, empirical mode decomposition (EMD) combined with HT is proposed to decompose the target signal into several IMFs by cubic spline interpolation (Huang *et al.* 1998). However, the EMD is not guaranteed theoretically and it has difficulties for the decomposition of closely-spaced frequency components (Lei *et al.* 2013, Zheng *et al.* 2017). By injecting a generated white noise into the original signal, ensemble empirical mode decomposition (EEMD) is capable of extracting closely-spaced frequency components. However, the decomposed results are sensitive to parameters selection, and pseudo components may be produced when improper parameters are selected (Chen and Cui 2016). The bilinear representations such as the Cohen and the affine class distributions can yield extremely precise IF estimation in the case of mono-component whose IF oscillates linearly, but it may fail in the multi-component situation because of interference terms (Flandrin *et al.* 1996, Padovese 2004, Hussain and Boashash 2002). Although considerable researches have demonstrated that TFA could be a perfect solution for processing non-stationary signals, but all TFA

*Corresponding author, Ph.D.

E-mail: X.We.3@warwick.ac.uk

^a Ph.D.

E-mail: liujingliang@fafu.edu.cn

^b Professor

E-mail: renhuiqiu@fafu.edu.cn

^c Graduate Student

E-mail: jyz365246@163.com

^d Ph.D. Student

E-mail: Yanjie.Zhu@warwick.ac.uk

^e Associate Professor

E-mail: I.Laory@warwick.ac.uk

methods have their own merits and deficiencies due to the complication of time-varying problem, and thus more relative studies need to be carried out (Peng *et al.* 2012).

Wavelet transform as an adaptive algorithm is particularly useful for analyzing periodic, noisy, intermittent and transient signals (Ni *et al.* 2017). The past two decades have witnessed its great success on parameter identification of time-varying structures. For example, Xu *et al.* (2012) combined wavelet theory and state-space method to identify dynamic parameters in linear time-varying systems. Hou *et al.* (2006) proposed a continuous wavelet-based technique for the identification of instantaneous modal parameters of time-varying structures. By transforming a time-varying identification problem into a time-invariant one, Su *et al.* (2014) employed continuous wavelet transform (CWT) to identify the instantaneous modal parameters in the frequency ranges of interest. However, the measured responses in ambient vibration tests are usually mixed with harmonic components and as a result CWT cannot be directly performed. To address this issue, Le and Argoul (2015) presented a time-frequency domain decomposition technique to distinguish harmonic components from structural modes in the operational modal identification. Yan and Ren (2013) also proposed a continuous-wavelet transmissibility method to extract the operational modal frequencies and mode shapes of a linear system. The simulation and real case application demonstrated that the proposed method is capable of identifying the operational modal parameters of full-sized structures. In addition, Kijewski and Kareem (2003) argued that civil engineering structures usually possess long period or low-frequency motions and thus require finer frequency resolution in the parent wavelet function.

Actually, the energy of a response signal concentrates around several curves in the time-frequency plane after CWT is performed. These concentrated bright curves in the wavelet scalogram are in fact the maxima points of wavelet coefficients and named ‘wavelet ridges’. Therefore, a successful extraction of wavelet ridges is crucial to identify instantaneous modal parameters of time-varying structures. The IF extraction from wavelet ridges in a way of phase information was first proposed by Delprat *et al.* (1992). However, the phase information is quite sensitive to noises, which limits its engineering application. The direct maximum ridge detection algorithm is such a method to extract wavelet ridges by detecting the maximum magnitude of wavelet coefficients for every discrete time points, but its practical application will inevitably be affected by a number of noise sources in engineering structures (Liu *et al.* 2004, Qin *et al.* 2017). Therefore, a more robust algorithm with a consideration of noise effect is required for wavelet ridge detection. The cost function method based on dynamic optimization is an effective tool to extract ridges, but the exhaustive searching is still computationally expensive. Carmona *et al.* (1997, 1999) proposed a new ridge detection algorithm which can efficiently extract single or multiple ridges in the modulus of a wavelet transform. The main concept of this new method is ‘crazy climber’, which is similar to the simulated annealing algorithm. Contrary to the simulated annealing,

the ‘crazy climber’ looks for all the local maxima instead of searching the global maxima only. However, the most important issue needs to be taken into account is the computational cost of those methods. Dynamic programming algorithm was first presented by Liebling *et al.* (2006) to find a ridge of maximum response through the wavelet scalogram. Nevertheless, a penalty function was introduced during the dynamic programming process to improve the accuracy of wavelet ridge extraction, which in turn increases the computational complexity. Wang *et al.* (2013) combined penalty function and dynamic optimization techniques to extract the wavelet ridges. This method suffers the same problem with the dynamic programming and the crazy climber algorithm, that is, the computation is much time-consuming. Recently, the synchrosqueezing wavelet transform (SWT) is presented by Daubechies *et al.* (2011) to decompose an arbitrary asymptotic signal into a linear superposition of several approximate harmonics. The SWT algorithm reallocates the energy in the frequency direction and hence suppresses the blur along the frequency axis, but it cannot achieve good resolution in the time domain. Li and Liang (2012) proposed a generalized synchrosqueezing transform (GST) approach to reduce the diffusion in both time and frequency dimensions for frequency modulated signals, but this algorithm can only work well when the phase function or modulation source of the frequency modulated signal is known beforehand. However, this assumption is not always satisfied in practical engineering applications. More details about the applications of the SWT method and its improved algorithms can be found in the references (Pham and Meignen 2017, Feng *et al.* 2015, Oberlin *et al.* 2015, Cao *et al.* 2016).

To enhance the accuracy of IF extraction from time-varying structural responses, we present a wavelet ridge extraction method based on a maximum gradient algorithm and a smoothing approach. In this method, an optimal route to trace the change of wavelet coefficients from the gradient perspective was investigated, with the searching scope was strictly restricted in a predetermined region of the time-frequency plane according to the wavelet scalogram. The new detected optimal path is denoted as wavelet ridge, based on which the IFs of time-varying structures is estimated. The extracted IFs are smoothed by a polynomial curve fitting and a threshold method to reduce the effects of random noises. Compared with other methods, the greatest advantage of the new method is its simplicity and computational efficiency, which is very useful in practical engineering. Unlike crazy climber or dynamic programming algorithms, the calculation of gradient can be done without difficulty and moreover the complex iteration process is avoided in the searching of maximum gradient.

The outline of this paper is arranged as follows. The wavelet transform is introduced in Section 2. The new wavelet ridge extraction method based on maximum gradient and smoothing algorithm is proposed in detail in Section 3. A numerical case study is presented in section 4 to illustrate the proposed method, followed by an experimental demonstration on a steel cable with linearly and sinusoidally varying tension forces in Section 5.

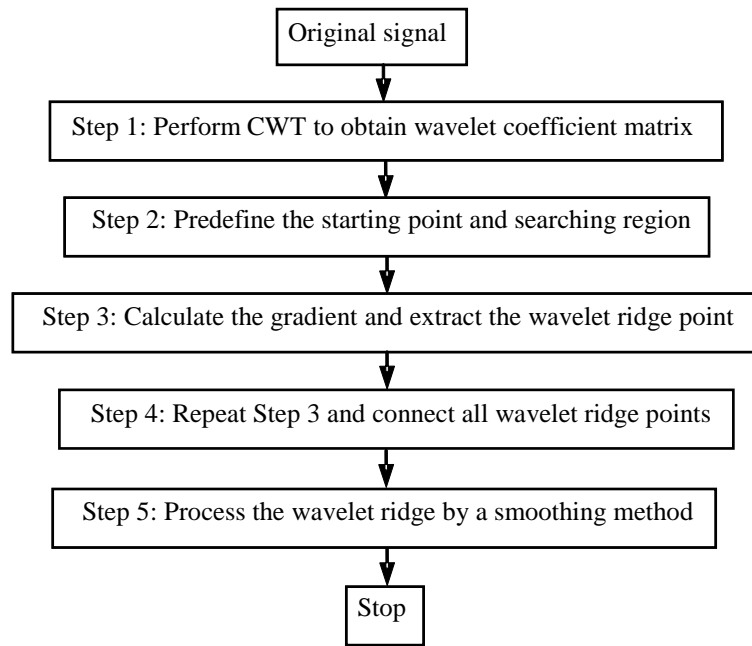


Fig. 1 The flowchart of the proposed method

The evaluation outcomes are summarized in conclusion section at the end of this paper.

2. Continuous wavelet transform

A nonstationary response signal of civil engineering structures usually consists of several components, and each one has individual local features. Usually, a multi-component signal can be expressed as a sum of n IMFs and a residual (Wang *et al.* 2013, Daubechies *et al.* 2011).

$$x(t) = \sum_{i=1}^n x_i(t) + r(t) \quad (1)$$

where each IMF is an oscillating function and denoted as a product of amplitude function and phase function, that is, $x_i(t) = A_i(t)\cos(\phi_i(t))$.

Extracting IFs of multi-component signals has been widely employed as a measure for structural health monitoring. A variety of signal processing techniques have developed for IF extraction, including the HT and CWT. While the HT is sensitive to random noises, CWT is suitable for coping with problems of more complicated local noises (Liu *et al.* 2004). In this paper, CWT is used to generate the wavelet scalogram of a signal before the extraction of wavelet ridge.

For a given square-integrable parent wavelet function ψ , the CWT of an arbitrary signal $x(t)$ is defined as

$$W_x(a, b) = \int_{-\infty}^{\infty} x(t) \frac{1}{\sqrt{a}} \overline{\psi\left(\frac{t-b}{a}\right)} dt \quad (2)$$

where a and b are the scale factor and the dilation factor, respectively, and $\overline{\psi\left(\frac{t-b}{a}\right)}$ represents the complex conjugate of $\psi\left(\frac{t-b}{a}\right)$. The wavelet coefficients $W_x(a, b)$ represent the similitude between the dilated parent wavelet and the signal at the time b and the scale a .

Morlet wavelet is chosen as parent wavelet function in this paper since its analog to the Fourier transform make it quite attractive for harmonic analysis and IF extraction. The mathematical expression of Morlet wavelet is as follows.

$$\psi_{\sigma}(t) = c_{\sigma} \pi^{-\frac{1}{4}} e^{-\frac{t^2}{2}} (e^{-i\sigma t} - \kappa_{\sigma}) \quad (3)$$

where $\kappa_{\sigma} = e^{-\frac{\sigma^2}{2}}$, which is defined by the admissibility criterion; c_{σ} is the normalization constant, which is expressed as

$$c_{\sigma} = (1 + e^{-\sigma^2} - 2e^{-\frac{3\sigma^2}{4}})^{-\frac{1}{2}} \quad (4)$$

The parameter σ in the Morlet wavelet allows trade between time and frequency resolutions. By changing the value of σ continuously, the central frequency and frequency band are changed and thus an optimum resolution is obtained.

3. Wavelet ridge extraction

The crucial issue for the IF identification using CWT is how to extract wavelet ridges effectively. In this paper, a method for wavelet ridge extraction is proposed by combining a maximum gradient method and a smoothing algorithm. The flowchart of the proposed method is presented in Fig. 1. In this method, the CWT is first

performed on a response signal and then the searching ranges are preliminarily defined based on the resultant wavelet scalogram. Given an initial frequency at the starting time, the search was conducted in the prescribed range with the search direction defined by the maximum gradient. Connecting all points with maximum gradient gives the wavelet ridges, from which the IFs are identified. Finally, a smoothing operation based on a polynomial curve fitting and a threshold method is performed to reduce the effect of random noises on the IF extraction.

3.1 The maximum gradient algorithm

After performing the wavelet transform on a response signal $x(t)$ expressed as Eq. (1), one can obtain the wavelet coefficients $W_x(a, b)$. These coefficients can be represented by a three-dimensional (3D) surface with b as the time axis, a as the scale axis and the modulus of wavelet coefficients as the height axis, as exemplified in Fig. 2. The wavelet ridges are the sequences of points with the maximum modulus i.e. the ridges of the 3-D surface. This indicates that a wavelet ridge is the curve of maximum gradient of the two-variable function $|W_x(a, b)|$, where $|\cdot|$ is the modulus of wavelet coefficients. In this paper, the IFs are extracted by calculating the curves of maximum gradient in a series of time-frequency sub-regions, each of which only includes a single wavelet ridge. The numerical calculation of maximum gradient curves is exemplified as follows.

Consider a real signal $x(t) = \cos(2\pi t + t^2)$. The sampling frequency is f_s and the length of the signal is n (the number of time points). Then the maximum gradient algorithm is described as follows.

(a) The CWT is first conducted on the signal $x(t)$. Let us assume that there are m discrete scales $[\widehat{a}_1, \widehat{a}_2, \widehat{a}_3, \dots, \widehat{a}_m]$ and n time points $[t_1, t_2, t_3, \dots, t_n]$. The resultant coefficient $W_x(a, b)$ is then a $m \times n$ matrix and the corresponding wavelet scalogram is plotted in Fig. 2.

(b) Based on the resultant wavelet scalogram, a sub-region of time-frequency plane, which includes the targeted IF curve, is identified as $[a_i^l, a_i^u]_{i=1,2,3,\dots,n}$. The scale at the i -th time instance is in the range of $[a_i^l, a_i^u]_{i=1,2,3,\dots,n}$.

(c) The search starts from a prescribed point S_1 , (a_1, t_1, W_x^1) on the 3D surface in the subregion, where t_1 is the initial time, a_1 is the scale at t_1 , and W_x^1 is the modulus of the corresponding wavelet coefficients. Correspondingly, the initial frequency can be calculated as $f_1 = F_c \cdot f_s / a_1$ in which F_c is the central frequency of parent wavelet function.

(d) It is assumed that the $(i-1)$ -th point on the ridge of the 3D surface in the prescribed sub-region has been found, denoted as S_{i-1} of the coordinate $(a_{i-1}, t_{i-1}, W_x^{i-1})$. The next step is to search the i -th point S_i , (a_i, t_i, W_x^i) in the prescribed sub-region $[a_i^l, a_i^u]$. Since t_i is known, a_i and W_x^i are the unknowns which will be determined by calculating the maxima among the gradients of lines relating the project of the point S_{i-1} on the time-scale plane.

The distance between S_{i-1} and S_i along the time axis can be defined as

$$D_i^t = |t_i - t_{i-1}| \quad (5)$$

For an arbitrary $a_i^j \in [\widehat{a}_1, \widehat{a}_2, \widehat{a}_3, \dots, \widehat{a}_m]$ at t_i , which is also restricted in the range of $[a_i^l, a_i^u]$, the distance between S_{i-1} and S_i along the scale axis is expressed as Eq. (6).

$$D_{i,j}^a = |a_i^j - a_{i-1}|_{a_i^j \in [a_i^l, a_i^u]} \quad (6)$$

Hence, the distance between S_{i-1} and S_i in the time-scale plane can be calculated as

$$D_{i,j}^H = \sqrt{(D_i^t)^2 + (D_{i,j}^a)^2} \quad (7)$$

Whereas the distance between S_{i-1} and S_i in the height direction at the scale a_i^j is denoted as

$$D_{i,j}^V = |W_x^{ij} - W_x^{i-1}| \quad (8)$$

where W_x^{ij} represents the wavelet coefficient corresponding to the time t_i and scale a_i^j .

Thereby, the gradient between S_{i-1} and S_i is computed according to Eqs. (7) and (8).

$$\tan\theta_i^j = D_{i,j}^V / D_{i,j}^H \quad (9)$$

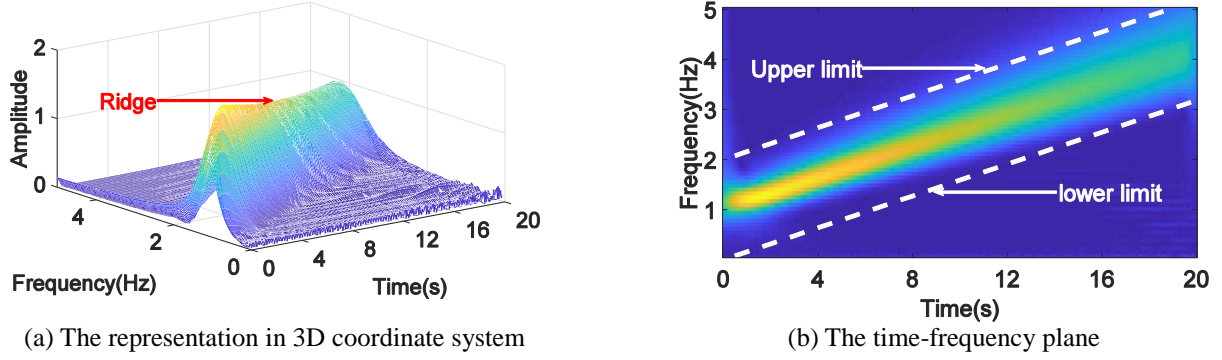
(e) The maximum gradient is the maximum value of $\tan\theta_i^j$ as displayed in Eq. (10). Then, the value of the scale corresponding to the maximum gradient $\tan\theta_i$ is calculated and assigned to a_i .

$$\tan\theta_i = \max_{a_i^l \leq a_i^j \leq a_i^u} |\tan\theta_i^j| \quad (10)$$

(f) The coefficients W_x^i at the point S_i can be found in the matrix $[W_x(a, b)]_{m \times n}$ because a_i is already solved and t_i is known in advance. Thus, the values at the point S_i , (a_i, t_i, W_x^i) , are totally recognized. After that, the frequency f_i can be computed easily by the formula $f = F_c \cdot f_s / a$.

(g) Repeat the searching step from (d) to (f) until the end of the signal. So far the frequencies at all points are solved by the maximum gradient (MG) method, which means the values at all points are recognized. Then, all points in the time-frequency plane are connected to a polyline, that is, the identified wavelet ridge.

The definition of initial frequency and the searching scope (usually divided by two parallel lines) is a key issue for the MG method. Although they can be determined in advance according to the time-frequency representation in the wavelet scalogram, the initial frequency and the searching scope really have a great impact on the accuracy of wavelet ridge extraction and IF identification. Therefore, the determination of initial frequency and the searching scope should be preset as precisely as possible. The MG algorithm can efficiently extract ridges from noiseless multi-component signals on condition that the multiple initial frequency and searching range are provided in advance. However, random noises are pervasive in practical

Fig. 2 The scalogram of the signal $x(t) = \cos(2\pi t + t^2)$

engineering structures, and it will inevitably affect the accuracy of the MG method. Therefore, it is necessary to introduce a new method to reduce the effect of noises and make the IF curves identified by the MG method smoother.

3.2 The smoothing algorithm

The IF identified by the MG method will be corrupted by random noises, especially at both ends of a response signal. To reduce the effect of random noises, a smoothing algorithm including a polynomial curve fitting method and a threshold algorithm is introduced. The process of polynomial curve fitting can be easily realized by the Matlab software, but the selection of the order of polynomial remains crucial for this algorithm. Typically, low order polynomial curves tend to be smooth while high order polynomial curves are liable to be lumpy. Because of this, an increase of the order/degree of polynomial does not always result in a better fit, and actually the selection of the degree depends on the problem to be solved. Here, a suggested value of 1 for the degree of the polynomial can provide a better fit for the signals with linearly varying IFs, but the corresponding value for the signals with sinusoidally varying IFs is recommended from 15 to 25.

Actually, the problem of noise contaminations can be formulated as Eq. (11).

$$f = w + r \quad (11)$$

where f is the noisy IF, w is the noise-free or exact frequency and r represents noises or estimation error. Our goal is to estimate w from the noisy observation f and the estimation is denoted as $\hat{w}(f)$. To reduce the influence of random noises, the hard threshold estimator (Chang *et al.* 2000, Han *et al.* 2007) is introduced and modified to smooth the IF identification results.

A new threshold operator $R_\lambda(k)$ is defined as Eq. (12).

$$R_\lambda(k) = \begin{cases} \lambda & \text{if } |k| > \lambda \\ k & \text{else} \end{cases} \quad (12)$$

where λ is the threshold defined in advance, k represents an independent variable. The value of k at the point S_i is defined as the changing rate of the frequency and expressed as Eq. (13).

$$k(i) = \frac{f_i - f_{i-1}}{t_i - t_{i-1}} \quad i = 2, 3, \dots, n \quad (13)$$

where f_i and f_{i-1} are the frequencies at time point t_i and t_{i-1} , respectively.

The choice of the threshold λ is delicate and important. Usually, a big threshold leads to a large bias of the estimator. On the other hand, a small threshold increases the variance of the smoother. Here, we empirically select λ by using Eq. (14).

$$\lambda = |\beta f'_a| = \beta \left| \frac{f_{max} - f_{min}}{t_{max} - t_{min}} \right| \quad (14)$$

where β is a self-defined coefficient and f'_a is denoted as the average changing rate of the frequency. f_{max} and f_{min} separately represent the maximum and minimum value of the noisy frequency in the time-frequency plane, and t_{max} and t_{min} are the time instants corresponding to f_{max} and f_{min} , respectively. Normally, f_{max} , f_{min} , t_{max} and t_{min} are estimated from the preliminary wavelet scalogram. The coefficient β in Eq. (14) has a great impact on the performance of the threshold algorithm and its value is selected as required. For the case of linearly varying IFs, the optimal value of β equals 1. Similarly, the proper value of β is recommended as $\pi/2$ in the case of IFs with sinusoidal variation, which can be interpreted as the following.

Typically, the response signal of a time-varying structure with its frequency oscillating sinusoidally can be expressed as Eq. (15).

$$y(t) = A \cos[B \sin(2\pi \alpha t) + \varphi] \quad (15)$$

where A , B , α , and φ are constants or slow-varying variables.

The frequency of $y(t)$ is calculated and expressed as Eq. (16).

$$f = 2\pi \alpha B \cos(2\pi \alpha t) \quad (16)$$

Thereby, f'_a , the average changing rate of the frequency, can be solved according to Eq. (16).

$$f'_a = \frac{f_{max} - f_{min}}{t_{max} - t_{min}} = \frac{2\pi \alpha B - (-2\pi \alpha B)}{T/2} = \frac{8\pi \alpha B}{T} \quad (17)$$

where T represents the period and it can be derived from

Eq. (16), that is

$$T = \frac{2\pi}{2\pi\alpha} = \frac{1}{\alpha} \quad (18)$$

Substitute Eq. (18) into Eq. (17) and yield

$$f'_a = 8\pi\alpha^2 B \quad (19)$$

Meanwhile, the exact changing rate of the frequency can be computed by taking a derivative of f denoted in Eq. (16) with respect to time.

$$f'_e = -4\pi^2\alpha^2 B \sin(2\pi\alpha t) \quad (20)$$

Therefore, the coefficient β can be calculated as Eq. (21).

$$\beta = |f'_e/f'_a| = \left| -\frac{\pi}{2} \sin(2\pi\alpha t) \right| \leq \frac{\pi}{2} \quad (21)$$

Since the threshold λ is determined by Eq. (14), the estimate of IF can be expressed as Eq. (22).

$$\hat{w}(f_i) = f_i = [t_i - t_{i-1}] \cdot R_\lambda(k) + f_{i-1} \quad (22)$$

So far the self-defined threshold algorithm has been accomplished and the effects of random noises can be suppressed to an extent, resulting in a more accurate estimation of IF.

4. Numerical example

To verify the performance of the proposed method on IF extraction, a numerical case of a multi-component signal with two frequency modulated (FM) components is considered. The target multi-component signal is defined as Eq. (23).

$$\begin{aligned} x(t) &= x_1(t) + x_2(t) \\ &= \cos[2.4\pi t + 0.8 \sin(0.4\pi t)] \\ &\quad + \cos[3.6\pi t + 0.5 \sin(0.5\pi t)] \end{aligned} \quad (23)$$

The frequencies of component signals $x_1(t)$ and $x_2(t)$ are as follows: $f_1 = d\phi_1/dt = 1.2 + 0.16 \cos(0.4\pi t)$ Hz, and $f_2 = d\phi_2/dt = 1.8 + 0.125 \cos(0.5\pi t)$ Hz. In this case, a sampling rate of 20 Hz is used and the total sampling time is set to be 12 seconds. To consider the impact of the noise, the signal $x(t)$ is assumed to be contaminated by a 20% Gaussian white noise, which means that the ratio of A_{noise}^2 to A_{signal}^2 is 20% where A_{signal} and A_{noise} are the root mean square values of the signal and the noise, respectively. Fig. 3 shows the signal contaminated by 20% Gaussian white noise.

The Morlet wavelet transform was performed on the noisy signal, with central frequency and frequency band set as 1 and 2 Hz, respectively. The result of the wavelet transform is presented in Fig. 4. It is apparent that there are two highlighted wavelet ridges or IF trajectories in the time-frequency domain, and each oscillates sinusoidally. More precisely, the IF of the component signal $x_1(t)$ varies from 1.1 to 1.4 Hz, while the IF value of $x_2(t)$ changes from 1.6 to 2.0 Hz. However, both two wavelet ridges suffer blur and thus need to be refined. According to the proposed MG

method, two searching regions are determined by two sets of parallel lines according to the IF trajectories displayed in the time-frequency plane. While the first region, ranging from 1.1 to 1.4 Hz, is indicated in Fig. 4 by two thick black dashed lines, the second region, ranging from 1.6 to 2.0 Hz, is indicated in Fig. 4 by two thick red dashed lines. The initial frequencies of $x_1(t)$ and $x_2(t)$ at $t=0$ are chosen to be 1.2 and 1.9 Hz, respectively. Then the wavelet ridges were extracted by the MG method and smoothed by a polynomial curve fitting and a threshold algorithm. The final results of IF identification are plotted in Fig. 5. It is shown that the identified IFs are in good agreement with their theoretical counterparts. Compared with the standard SWT algorithm, the proposed method can extract the IF of each component with higher accuracy if the searching scope and the initial values of the initial frequencies of $x_1(t)$ and $x_2(t)$ is accurately defined in advance.

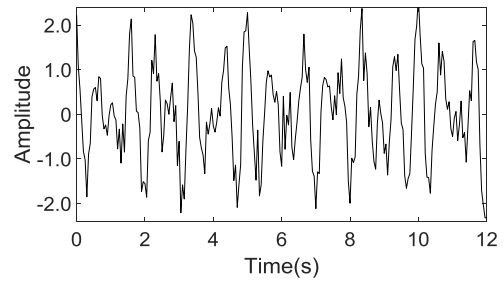


Fig. 3 The simulated multi-component signal with 20% Gaussian white noise

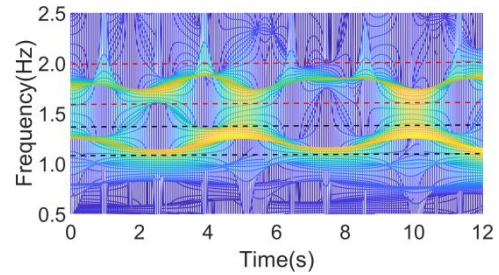


Fig. 4 The wavelet scalogram of the multi-component signal with 20% Gaussian white noise

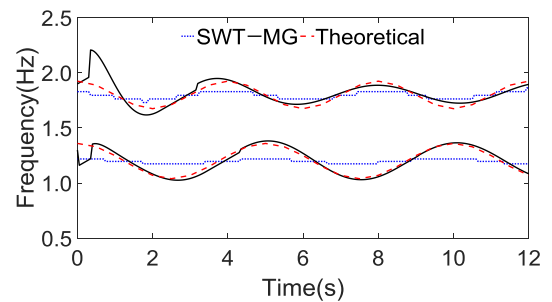


Fig. 5 The IFs of the multi-component signal extracted by the MG and SWT methods

5. Experimental case study

To further validate the accuracy of the proposed method, a cable composed of $7\Phi 5$ steel wires is considered. The cable has elastic modulus $E=1.95\times 10^5$ MPa, area of cross section $A=1.374\times 10^4$ m² and density of unit length $q=1.1$ kg/m. The stiffness of the cable is changed due to the applied time-varying tension forces so that the natural frequency of the cable is time-dependent. The cable is fixed at one end, and the other end is connected to a MTS loading system. The total length of cable between two ends is 4.55m. The accelerometer is installed vertically at the mid-point of the cable. The test setup is shown in Fig. 6.

During the cable test, an initial constant pretension force was firstly applied by MTS load actuator to the cable. When the test setup and data collection were ready, the cable tension force was changed continuously using the MTS load system. At the same time, the impact hammer is used to generate free vibration and the vertical acceleration response was recorded at a sampling frequency of 600 Hz. The tension force with linear or sinusoidal change was considered during the test. The theoretical IFs of the cable were obtained by solving eigenvalues and eigenvectors of vibration equations, assuming that the parameters of cable keep invariant over a relatively short time interval, which is designated as the time frozen method (Wang *et al.* 2013). For simplicity, only the fundamental frequencies of the cable at several fixed tension forces were considered at this case and thus listed in Table 1. Other theoretical fundamental frequencies at different fixed tension forces can be computed using linear interpolation algorithm, which can be used as theoretical IFs to compare with the extracted IFs under time-varying tension forces in the following cases.

For the first case, the initial tension force of the cable was 20 kN, and then the tension force increased linearly at the rate of 1.67 kN/s using the MTS load system.

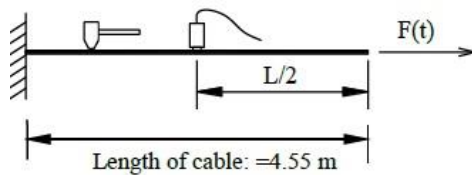


Fig. 6 The cable test setup

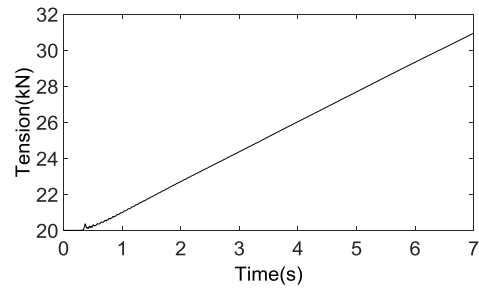


Fig. 7 The measured cable tension forces with linear variation

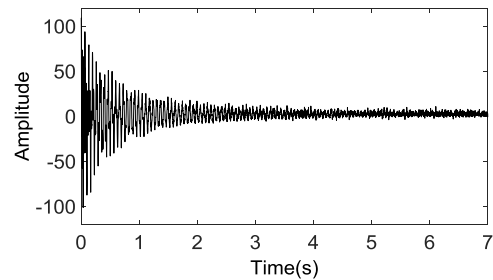


Fig. 8 The measured cable acceleration responses with linearly varying tension forces

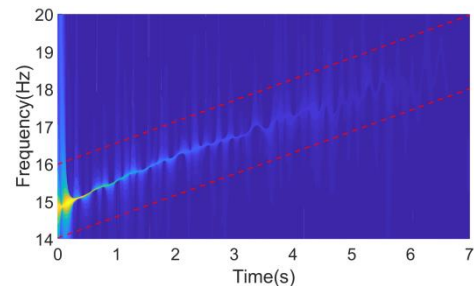


Fig. 9 The wavelet scalogram of the cable acceleration responses with linearly varying tension forces

The duration of data acquisition was 7s. The measured tension force and acceleration responses were shown in Figs. 7 and 8, respectively.

By performing Morlet wavelet transform on the acceleration responses, a wavelet scalogram was obtained and displayed in Fig. 9, which indicates that the first order IF curve varies linearly in the range of 14 to 20 Hz. Here, the central frequency and frequency bandwidth of Morlet wavelet function were selected as 1 and 2 Hz, respectively. Then, two red dashed lines in parallel with the IF trajectories were selected as the upper and lower limit of the searching range, respectively.

The initial frequency was set as 15 Hz. After that, the searching and smoothing algorithms were implemented to extract the IFs of the cable and the theoretical fundamental natural frequencies solved by the time frozen method are shown in Table 2.

Table 1 The theoretical fundamental frequency of the cable under different constant tensions

Tension (kN)	13.0	15.0	17.0	19.0	20.0	20.3	20.6	20.9	21.2
Frequency (Hz)	12.26	13.08	13.87	14.65	15.03	15.13	15.24	15.33	15.45
Tension (kN)	21.5	21.8	22.0	22.5	23.0	23.5	24.0	24.5	25.0
Frequency (Hz)	15.56	15.67	15.70	15.91	16.09	16.24	16.41	16.54	16.72
Tension (kN)	25.5	26.0	26.5	27.0	27.5	28.0	29.0		
Frequency (Hz)	16.88	17.03	17.19	17.33	17.47	17.63	17.90		

Table 2 The theoretical modal frequency of the cable with linearly varying tension forces

Time (s)	0	0.06	0.43	0.62	0.78	0.97	1.15	1.26	1.55
Tension (kN)	20.0	20.3	20.6	20.9	21.2	21.5	21.8	22.0	22.5
Frequency (Hz)	15.03	15.13	15.24	15.33	15.45	15.56	15.67	15.70	15.91
Time (s)	1.85	2.15	2.46	2.76	3.06	3.35	3.65	3.96	4.26
Tension (kN)	23.0	23.5	24.0	24.5	25.0	25.5	26.0	26.5	27.0
Frequency (Hz)	16.09	16.24	16.41	16.54	16.72	16.88	17.03	17.19	17.33
Time (s)	4.56	4.96	5.47	6.09	6.7				
Tension (kN)	27.5	28.0	29.0	30.0	31.0				
Frequency (Hz)	17.47	17.63	17.90	18.20	18.47				

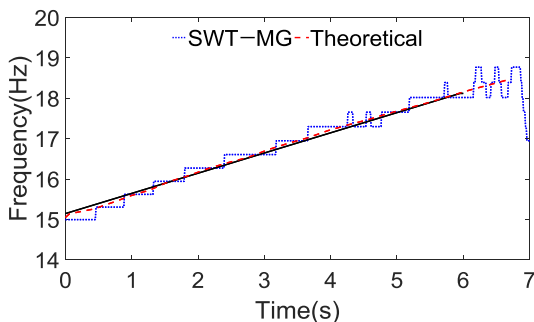


Fig. 10 The extracted IF of the cable with linearly varying tension forces

Fig. 10 presented the corresponding theoretical fundamental frequencies together with the extracted IFs using the MG method and SWT, respectively. It is shown in Fig. 10 that the MG method can extract IFs of the cable subjected to a linearly increased tension force more accurately than standard SWT.

In the second case, the initial tension force of the cable was set to 22 kN, and then the tension force changed sinusoidally, which is shown in Fig. 11. The measured acceleration responses with a duration of 6 seconds is given in Fig. 12.

As did in the first case, the Morlet wavelet transform was performed on the acceleration response signal with the central frequency and frequency bandwidth set as 1 and 2 Hz, respectively. The wavelet scalogram was plotted in Fig. 13. As can be seen in Fig. 13, the fundamental modal frequency oscillates sinusoidally. Then, the searching scope

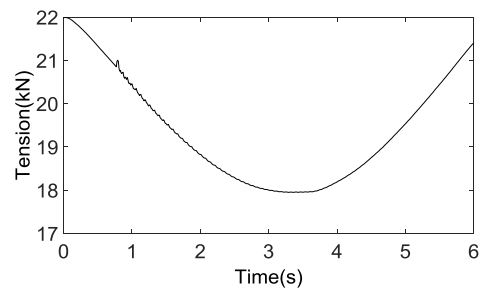


Fig. 11 The measured cable tension forces with sinusoidal variation

in the MG method was restricted by two parallel lines (red thick dashed lines) and plotted in Fig. 13, with the frequencies of the two lines set as 14 and 16 Hz, respectively. The searching step was then conducted with the initial frequency defined as 15.7 Hz on the basis of the estimation from the wavelet scalogram. Eventually, the IF extracted by the MG method was smoothed by a polynomial curve fitting and a threshold algorithm and the corresponding results were displayed in Fig. 14. By using the time frozen method the theoretical fundamental natural frequencies are solved and shown in Table 3. The comparison of theoretical fundamental modal frequencies and IF identification results presented in Fig. 14 indicates that the identified IFs using the MG method are in reasonable accordance with theoretical results. Compared with the standard SWT, the MG method provides better time-frequency resolutions on IF extraction of a cable with sinusoidal tension forces.

Table 3 The theoretical modal frequency of the cable with sinusoidally varying tension forces

Time (s)	0	0.2	0.4	0.6	0.9	1.2	1.8	2.1	2.5
Tension (kN)	22.00	21.84	21.55	21.17	20.59	20.09	19.10	18.71	18.3
Frequency (Hz)	15.70	15.68	15.58	15.44	15.24	15.06	14.69	14.54	14.38
Time (s)	3.1	3.4	3.8	4.2	4.7	5.3	5.4	5.6	5.9
Tension (kN)	17.98	17.96	18.03	18.37	19.03	20.06	20.25	20.63	21.22
Frequency (Hz)	14.25	14.24	14.27	14.40	14.66	15.05	15.11	15.25	15.46
Time (s)	6.0								
Tension (kN)	21.42								
Frequency (Hz)	15.53								

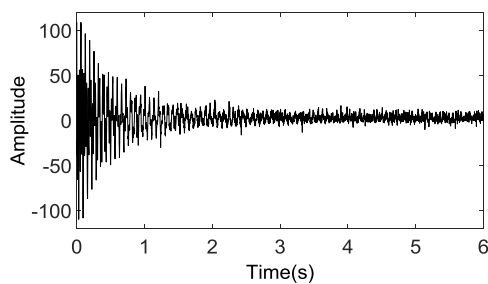


Fig. 12 The measured cable acceleration responses with sinusoidally varying tension forces

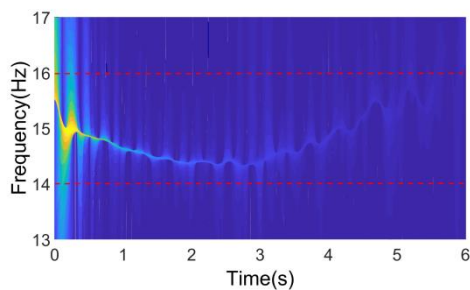


Fig. 13 The wavelet scalogram of the cable acceleration responses with sinusoidally varying tension forces

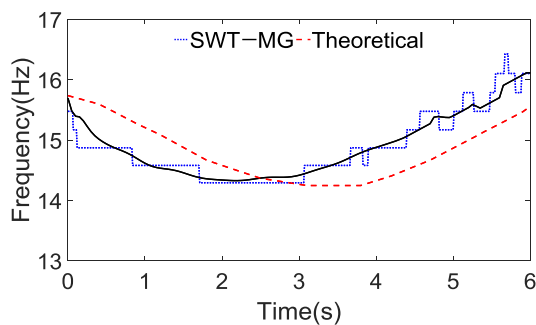


Fig. 14 The extracted IF of the cable with sinusoidally varying tension forces

6. Conclusions

This paper presents a method for IF extraction of time-varying structures, which are frequently encountered in the field of civil engineering. The proposed method is a combination of the MG method and a smoothing method. The method can successfully extract wavelet ridges from response signals by searching an optimal path on a 3D surface. Starting from an initial frequency, the search proceeds in a prescribed range along the direction defined by the maximum gradient at every time points. The IFs extracted by the MG method are smoothed by using a polynomial curve fitting method and a self-defined threshold algorithm such that the effect of random noises on identified time-frequency curves is alleviated. The proposed method is demonstrated using a numerical example and an experimental case study. The results demonstrate that the method can accurately identify not only the IFs of multi-component numerical signals but also those of the signals from practical time-varying structures. In addition, the proposed method performs better than the standard SWT, provided that the searching area and initial frequency are precisely predetermined.

Acknowledgments

This study is sponsored by the National Natural Science Foundation of China (NSFC) under Grants No.51608122, Natural Science Foundation of Fujian Province under Grants No.2016J05111 and the Outstanding Youth Fund of Fujian Agriculture and Forestry University under Grants No. XJQ201728, China Postdoctoral Science Foundation under Grants No. 2018M632561 and the China Scholarship Council (CSC) (No. 201708350021). We also thank Dr. Wang Chao of Huazhong University of Science and Technology and Professor Wei-Xin Ren of Hefei University of Technology for providing us the data of a cable test with time-varying tension forces. The results and opinions expressed in this paper are those of the authors only.

References

- Cao, H., Xi, S., Chen, X. and Wang, S. (2016), "Zoom synchrosqueezing transform and iterative demodulation: Methods with application", *Mech. Syst. Signal Pr.*, **2016**, **72-73**, 695-711.
- Carmona, R., Hwang, W.L. and Torr sani, B. (1997), "Characterization of signals by the ridges of their wavelet transforms", *T. Signal Pr.*, **45**(10), 2586-2590.
- Carmona, R., Hwang, W.L. and Torr sani, B. (1999), "Multi-ridge detection and time-frequency reconstruction", *IEEE T. Signal Process.*, **47**(2), 480-492
- Chang, S.G., Yu, B. and Vetterli M. (2000), "Adaptive wavelet thresholding for image denoising and compression", *IEEE T. Image Processing*, **9**(9), 1532-1546.
- Chen, X. and Cui, B. (2016), "Efficient modeling of fiber optic gyroscope drift using improved EEMG and extreme learning machine", *Signal Process.*, **128**, 1-7.
- Daubechies, I., Lu, J.F. and Wu, H.T., (2011), "Synchrosqueezed wavelet transforms: An empirical mode decomposition-like tool", *Appl. Comput. Harmon. A.*, **30**(2), 243-261.
- Delprat, N., Escudie, B., Guillemain, P., Kromland-Martinet, R., Tchamitchian, P. and Torrain, B. (1992), "Asymptotic wavelet and Gabor analysis: extraction of instantaneous frequencies", *IEEE T. Inform. Theory*, **38**(2), 644-664.
- Feldman, M. (1994a), "Non-linear system vibration analysis using Hilbert transform-I: free vibration analysis method FREEVIB", *Mech. Syst. Signal Pr.*, **8**(2), 119-127.
- Feldman, M. (1994b), "Non-linear system vibration analysis using Hilbert transform-II: forced vibration analysis method FORCEVIB", *Mech. Syst. Signal Pr.*, **8**(3), 309-318.
- Feldman, M. and Braun, S. (2017), "Nonlinear vibrating system identification via Hilbert decomposition", *Mech. Syst. Signal Pr.*, **84**, 65-96.
- Feng, Z., Chen, X. and Liang, M. (2015), "Iterative generalized synchrosqueezing transform for fault diagnosis of wind turbine planetary gearbox under nonstationary conditions", *Mech. Syst. Signal Pr.*, **52**, 360-375.
- Feng, Z., Liang, M. and Chu, F. (2013), "Recent advances in time-frequency analysis methods for machinery fault diagnosis: A review with application examples", *Mech. Syst. Signal Pr.*, **38**, 165-205.
- Flandrin, P. and Goncalves, P. (1996), "Geometry of affine time-frequency distributions", *Appl. Comput. Harmon. A.*, **3**(1), 10-39.
- Han, M., Liu, Y., Xi, J. and Guo, W. (2007), "Noise smoothing for nonlinear time series using wavelet soft threshold", *IEEE Signal Proc. Lett.*, **14**(1): 62-65.
- Hou, Z., Hera, A. and Shinde, A. (2006), "Wavelet-based structural health monitoring of earthquake excited structures", *Comput.-Aided Civil Infrastruct. Eng.*, **21**(4), 268-79.
- Huang, N.E., Shen, Z., Long, S.R., Wu, M.C., Shih, H.H. and Zheng, Q. (1998), "The empirical mode decomposition and Hilbert spectrum for nonlinear and nonstationary time series analysis", *P. R. Soc. London-Series*, **454**(1971), 903-995.
- Hussain, Z.M. and Boashash, B. (2002), "Adaptive instantaneous frequency estimation of multicomponent FM signals using quadratic time-frequency distributions", *IEEE T. Signal Process.*, **50**(8), 1866-1876.
- Kijewski, K. and Kareem, A. (2003), "Wavelet transforms for system identification in civil engineering", *Comput.-Aided Civil Infrastruct. Eng.*, **18**(5), 339-355.
- Le, T.P. and Argoul, P. (2015), "Distinction between harmonic and structural components in ambient excitation tests using the time-frequency domain decomposition technique", *Mech. Syst. Signal Pr.*, **52-53**, 29-45.
- Lei, Y., Lin, J., He, Z. and Zuo, M.J. (2013), "A review on empirical mode decomposition in fault diagnosis of rotating machinery", *Mech. Syst. Signal Pr.*, **35**, 108-126.
- Li, C. and Liang, M. (2012), "A generalized synchrosqueezing transform for enhancing signal time-frequency representation", *Signal Process.*, **92**(9), 2264-2274.
- Liebling, M., Bernhard, T.F., Bachmann, A.H., Froehly, L., Lasser, T. and Unser, M. (2005), "Continuous wavelet transform ridge extraction for spectral interferometry imaging". *Proceedings of the SPIE, Coherence Domain Optical Methods and Optical Coherence Tomography in Biomedicine IX*, San Jose, CA, USA, April.
- Liu, H., Cartwright, A.N. and Basaran, C. (2004), "Moir  interferogram phase extraction: a ridge detection algorithm for continuous wavelet transforms", *Appl. Optics*, **43**(4), 850-857.
- Liu, J.L., Wang, Z.C., Ren, W.X. and Li, X.X. (2015), "Structural time-varying damage detection using synchrosqueezing wavelet transform", *Smart Struct. Syst.*, **15**(1), 119-133.
- Ni, S.H., Yang, Y.Z. and Tsai, P.H. (2017), "Evaluation of pile defects using complex continuous wavelet transform analysis", *NDT&E Int.*, **87**, 50-59.
- Oberlin, T., Meignen, S. and Perrier, V. (2015), "Second-order synchrosqueezing transform or invertible reassignment? Towards ideal time-frequency representations", *IEEE T. Signal Process.*, **63**(5), 1335-1344.
- Padovese, L.R. (2004), "Hybrid time-frequency methods for non-stationary mechanical signal analysis", *Mech. Syst. Signal Pr.*, **18**, 1047-1064.
- Peng, Z.K., Zhang, W.M., Lang, Z.Q., Meng, G. and Chu, F.L. (2012), "Time-frequency data fusion technique with application to vibration signal analysis", *Mech. Syst. Signal Pr.*, **29**, 164-173.
- Pham, D.H. and Meignen, S. (2017), "High-order synchrosqueezing transform for multicomponent signals analysis-with an application to gravitational-wave signal", *IEEE T. Signal Process.*, **65**(12), 3168-3177.
- Qin, Y., Mao, Y. and Tang, B. (2017), "Multicomponent decomposition by wavelet modulus maxima and synchronous detection", *Mechanic Syst. Signal Pr.*, **91**, 57-80.
- Shi, Z.Y., Law, S.S. and Xu, X. (2009), "Identification of linear time-varying mdof dynamic systems from forced excitation using Hilbert transform and EMG method", *J. Sound Vib.*, **321**, 572-589
- Su, W.C., Liu, C.Y. and Huang, C.S. (2014), "Identification of instantaneous modal parameter of time-varying systems via a wavelet-based approach and its application", *Comput.-Aided Civil Infrastruct. Eng.*, **29**(4), 279-298.
- Wang, C., Ren, W.X., Wang, Z.C. and Zhu H.P., (2013), "Instantaneous frequency identification of time-varying structures by continuous wavelet transform", *Eng. Struct.*, **52**(9), 17-25.
- Xu, X., Shi, Z.Y. and You, Q. (2012), "Identification of linear time-varying systems using a wavelet-based state-space method", *Mech. Syst. Signal Pr.*, **26**, 91-103.
- Yan, W.J. and Ren, W.X. (2013), "Use of continuous-wavelet transmissibility for structural operational modal analysis", *J. Struct. Eng.*, **139**(9), 1444-1456.
- Zheng, J., Pan, H., Yang, S. and Cheng, J. (2017), "Adaptive parameterless empirical wavelet transform based time-frequency analysis method and its application to rotor rubbing fault diagnosis", *Signal Process.*, **130**, 305-314.